

# Evaluation of an Ionic Porous Organic Polymer for Water Remediation

Shaoshao Jiao, Liming Deng, Xinghao Zhang, Yaowen Zhang, Kang Liu,\* Shaoxiang Li, Lei Wang, and Dingxuan Ma\*



Cite This: *ACS Appl. Mater. Interfaces* 2021, 13, 39404–39413



Read Online

ACCESS |

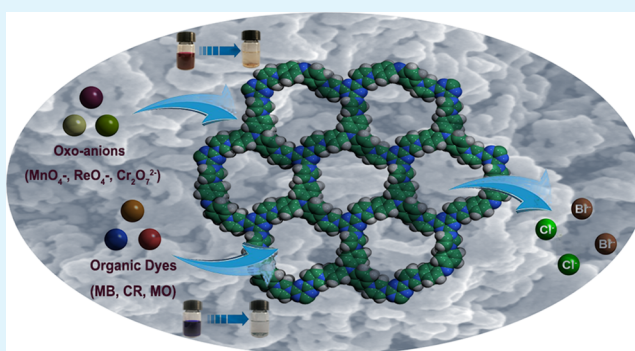
Metrics & More

Article Recommendations

Supporting Information

**ABSTRACT:** The targeted synthesis of a novel ionic porous organic polymer (iPOP) was reported. The compound (denoted as QUST-iPOP-1) was built up through a quaternization reaction of tris(4-imidazolylphenyl)amine and cyanuric chloride, and then benzyl bromide was added to complete the quaternization of the total imidazolyl units. It featured a special exchangeable  $\text{Cl}^-/\text{Br}^-$ -rich structure with high permanent porosity and wide pore size distribution, enabling it to rapidly and effectively remove environmentally toxic oxo-anions including  $\text{Cr}_2\text{O}_7^{2-}$ ,  $\text{MnO}_4^-$ , and  $\text{ReO}_4^-$  and anionic organic dyes with different sizes including methyl blue, Congo red, and methyl orange from water. Notably, QUST-iPOP-1 showed ultra-high capacity values for radioactive  $\text{TcO}_4^-$  surrogate anions ( $\text{MnO}_4^-$  and  $\text{ReO}_4^-$ ),  $\text{Cr}_2\text{O}_7^{2-}$ , methyl blue, and Congo red, and these were comparable to some reported compounds of exhaustive research. Furthermore, the relative removal rate was high even when other concurrent anions existed.

**KEYWORDS:** cationic porous organic polymer, anionic pollutants, organic pollutants, adsorption, selectivity



## INTRODUCTION

Water pollution has become an environmental and public issue of great concern, and remediation of toxic contaminants including heavy metal ions and organic dyes has attracted research attention worldwide.<sup>1–3</sup> These pollutants discharged from printing, electroplating, textile, paper, and leather industries as well as radioactive pollutants produced by nuclear reactors have turned into an urgent challenge as they were omnipresent in the affected areas. The oxo-anions in water are the chief pollutants on the basis of the U.S. Environmental Protection Agency.<sup>4</sup> Especially, heavy-metal ion Cr(VI)-derived oxo-anions have served harm to human health, and thus the International Agency for Research on Cancer has included them as a group 1 carcinogenic chemical for human.<sup>5–8</sup> In addition, <sup>99</sup>Tc is a problematic radionuclide from the nuclear industry with a long half-life ( $2.13 \times 10^5$  years) and exists primarily as a pertechnetate ( $\text{TcO}_4^-$ ) ion. It is a great challenge to carry out  $\text{TcO}_4^-$ -contaminated environmental restoration due to its high solubility in water and strong mobility.<sup>9–11</sup> Considering its radioactivity and the operational difficulties, perrhenate ( $\text{ReO}_4^-$ ) and permanganate ( $\text{MnO}_4^-$ ) anions were employed as the nonradioactive surrogates for  $\text{TcO}_4^-$ . Furthermore, the wastewater from printing and dyeing containing teratogenic and carcinogenic compounds, especially complex aromatic compounds, is difficult to purify thoroughly by bioprocessing. The aquatic environmental safety and human

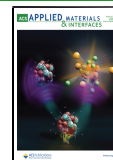
health have been directly threatened by the dyeing wastewater.<sup>12–14</sup>

So far, many techniques have been used to eliminate toxic contaminants from wastewater, such as electrocatalysis/photocatalysis,<sup>15,16</sup> chemical precipitation,<sup>17,18</sup> biotreatment,<sup>19,20</sup> membrane separation,<sup>21,22</sup> adsorption,<sup>23,24</sup> and so on.<sup>25–29</sup> Among these technologies, adsorption is considered to be a more effective method due to its low cost, high feasibility, relatively simple and safe operation, and efficient performance even for wastes with low concentrations of pollutants.<sup>30–34</sup> Hence, porous materials including zeolites, activated carbons, cellulose derivatives, metal–organic frameworks (MOFs), covalent organic frameworks (COFs), etc. have become increasingly important for water purification.<sup>35–38</sup> However, the shortcomings of these materials like the low adsorption capacity of zeolites, activated carbons, and cellulose derivatives; complicated preparation of most COFs; and relatively poor water stability of MOFs limit their applications. Therefore, developing a novel solid sorbent for efficient and rapid

Received: June 5, 2021

Accepted: August 3, 2021

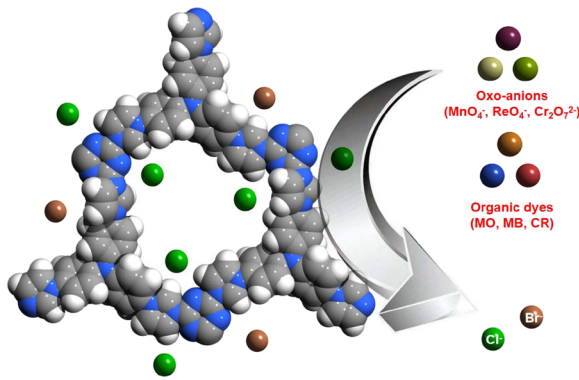
Published: August 13, 2021



sequestration of contaminants from wastewater still remains an ongoing challenge.

Porous organic polymers (POPs) are a burgeoning type of porous materials with microporous or mesoporous structures formed by covalent bonding of organic structural units, which have clear advantages such as a large specific surface area, low skeleton density, good thermal stability and chemical stability, simple and diverse synthetic methods, and adjustable and designable pore properties.<sup>39–42</sup> These compounds have received wide attention due to their own characteristics and have excellent performance and potential application value in gas adsorption storage,<sup>43–47</sup> heterogeneous catalysis,<sup>48–53</sup> photovoltaic materials,<sup>54–57</sup> and chemical biosensors,<sup>58–61</sup> but they are relatively rarely used for removing ionic contaminants from water.<sup>62,63</sup> Ionic porous organic polymers (iPOPs) represent a small fraction of the POP family and are much less-explored than neutral POPs.<sup>64–69</sup> Recently, a series of iPOPs have been designed and synthesized, which show more excellent adsorption performance when removing inorganic ionic contaminants and organic ionic dyes in water because of the strong interaction between the adsorbent and the framework.<sup>70–74</sup> Performing anion capture by ion exchange, a cation network with exchangeable anions is a major requirement. Due to their structural diversity and chemical stability, cationic porous organic polymers are very suitable for capturing harmful anionic pollutants from water, while less directly synthesizing cationic POPs were reported to date for detection of anions in water.<sup>75,76</sup> Therefore, we report the novel ionic porous organic polymer QUST-iPOP-1, which was facilely synthesized by a one-step process from tri(4-imidazolylphenyl)amine and cyanuric chloride (Scheme 1). As

**Scheme 1.** Space-Filling View of QUST-iPOP-1 in an Amorphous Periodic Cell and Schematic of the Oxo-Anions and Organic Dye Capture (Gray: C, White: H, Blue: N, Green: Cl, and Brown: Br)



a result, QUST-iPOP-1 exhibits good adsorption properties for removing anionic pollutants from water and shows extremely high adsorption capacities for radioactive TcO<sub>4</sub><sup>-</sup> surrogate anions (MnO<sub>4</sub><sup>-</sup> and ReO<sub>4</sub><sup>-</sup>), Cr<sub>2</sub>O<sub>7</sub><sup>2-</sup>, methyl blue, and Congo red.

## EXPERIMENTAL SECTION

**General Methods.** Tri(4-imidazolylphenyl)amine (TIPA) was prepared according to a literature method.<sup>77</sup> Other chemicals and solvents are analytically pure and are commercially available. Elemental analyses were performed on a Vario EL III Elemental Analyzer. Powder X-ray diffraction (PXRD) patterns were recorded in a range of  $2\theta = 5\text{--}50^\circ$  on a desktop X-ray diffractometer (RIGAKU

D-MAX 2500/PC) with Cu K $\alpha$  radiation ( $\lambda = 1.5406 \text{ \AA}$ ). Thermogravimetric analysis (TGA) was measured on a Perkin-Elmer STA 6000 thermogravimetric analyzer between 30 and 800 °C under a N<sub>2</sub> atmosphere with a heating rate of 5 °C min<sup>-1</sup>. All infrared (IR) spectra were detected using a NICOLET 6700 FT-IR spectrophotometer by using KBr pellets in a range of 400–4000 cm<sup>-1</sup>. Solid-state <sup>13</sup>C NMR data were obtained using an Agilent DD2 600 MHz spectrometer. The X-ray photoelectron spectroscopy was tested on an ESCALAB 250Xi instrument. The zeta potential test was carried out on a zeta potential tester (WT, Malvern Instruments Co., Ltd., UK).

Liquid UV-vis spectroscopic analyses were characterized using a Shimadzu UV 2600 Spectrophotometer. A scanning electron microscope (SEM, S4800, Hitachi) and transmission electron microscope (TEM, JEM-2100F) were used to investigate the morphology and structure information of the as-prepared samples. The chemical compositions of the obtained samples were evaluated by X-ray photoelectron spectroscopy (Kratos Axis ULTRA), and the C 1s peak at 284.8 eV was used as an internal standard.

**Synthesis of the Exchange Material QUST-iPOP-1.** QUST-iPOP-1 was synthesized through a quaternization reaction. TIPA (0.80 mmol, 355 mg) was dissolved in 20 mL of DMF to obtain solution A. Cyanuric chloride (0.60 mmol, 270 mg) was dissolved in 20 mL of DMF to obtain solution B, and then solution A was slowly dropped into solution B during the mixing process. After stirring the mixture at 100 °C for 24 h, the reactor was cooled to room temperature and benzyl bromide (1 mL) was added. Then, the mixture was kept at 80 °C for an additional 7 h. When the reaction was completed, the precipitate was collected by centrifugation; washed successively with dimethylformamide (DMF), MeCN, tetrahydrofuran (THF), water, dichloromethane (DCM), and diethyl ether; and then exchanged the guest molecules with methanol (MeOH) for 3 days. The yellow-colored compound was filtered off and dried under vacuum at 60 °C for 12 h (Figure 1). Yield: 210 mg. FTIR (KBr, cm<sup>-1</sup>): 1630 (vw), 1540 (m), 1510 (m), 1485 (m), 1410 (vw), 1340 (vs), 1200 (s), 1054 (m), 962 (s), 816 (m), 711 (s), 612 (vs), 547 (s). Elemental analysis for QUST-iPOP-1: C, 46.06%; H, 5.09%; and N, 10.28%.

**Procedures for the Oxo-Anion Exchange and Time-Dependent Study.** In the case of anion exchanges of Cr<sub>2</sub>O<sub>7</sub><sup>2-</sup>, QUST-iPOP-1 (2 mg) was dispersed in a 4 mL K<sub>2</sub>Cr<sub>2</sub>O<sub>7</sub> aqueous solution (0.55 mmol L<sup>-1</sup> for Cr<sub>2</sub>O<sub>7</sub><sup>2-</sup>), and the mixture was gently shaken at room temperature for 2 min. Based on the typical absorption peaks of Cr<sub>2</sub>O<sub>7</sub><sup>2-</sup> at 257 and 350 nm, the degree of anion exchange was monitored by liquid UV-vis spectroscopy for solutions with different adsorption times. In a similar way, we measured the UV-vis spectra of MnO<sub>4</sub><sup>-</sup> and ReO<sub>4</sub><sup>-</sup> ions by using KMnO<sub>4</sub> and NH<sub>4</sub>ReO<sub>4</sub> aqueous solutions based on the typical absorption peaks (525 and 545 nm for MnO<sub>4</sub><sup>-</sup>; 205 and 230 nm for ReO<sub>4</sub><sup>-</sup>). Furthermore, the removal rate and concentration decays of the oxo-anions versus time were calculated from the time-dependent study. Moreover, the pseudo-first-order kinetic model and pseudo-second-order model kinetic model were used for kinetics data of oxo-anions to be fitted in Table S1 and Figure S7.

**Selective Adsorption Experiments.** In order to study the adsorption of the target ion in the presence of competing ions, we selected Cl<sup>-</sup>, Br<sup>-</sup>, NO<sub>3</sub><sup>-</sup>, and SO<sub>4</sub><sup>2-</sup> ions, which are common in wastewater. We prepared KCl, KBr, KNO<sub>3</sub>, and K<sub>2</sub>SO<sub>4</sub> solutions at a concentration of 50 mM. The concentration of the competing ionic solution is 100 times higher than the concentration of the target ionic solution, which better simulates the reality. For example, 4 mL of a 0.5 mM KMnO<sub>4</sub> solution was thoroughly mixed with 4 mL of a 50 mM KCl solution and then added and allowed to stand for 24 h.

Finally, the solid particles were filtered off from the solution and the liquid UV-vis spectra were recorded. In the same manner, KMnO<sub>4</sub> solution was mixed with KBr, KNO<sub>3</sub>, and K<sub>2</sub>SO<sub>4</sub> solutions, respectively, and 2 mg of the polymer was added. The K<sub>2</sub>Cr<sub>2</sub>O<sub>7</sub> solution and the (NH<sub>4</sub>)<sub>2</sub>ReO<sub>4</sub> solution were carried out as described above.

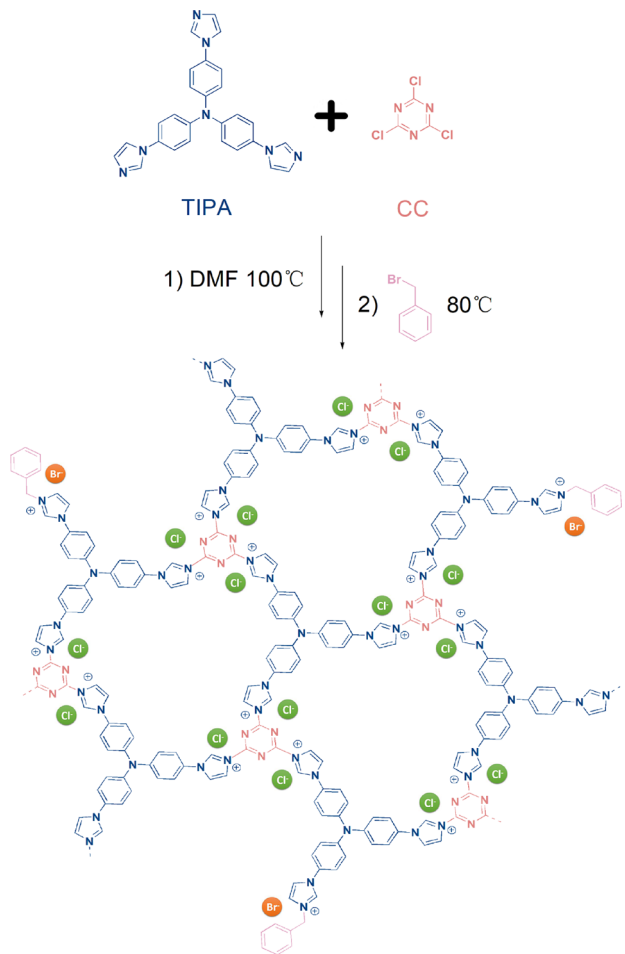


**Figure 1.** Synthesis routes and possible fragments of QUST-iPOP-1.

**Procedures for the Dye Exchange and Time-Dependent Study.** Two common kinds of dyes were selected for experiments, including positively charged methylene blue (MBL), rhodamine B (RhB), negatively charged methyl blue (MB), methyl orange (MO), and Congo red (CR).

Take dye exchange of MB as an example, QUST-iPOP-1 (2 mg) was dispersed in 6 mL of MB solution (60 mg/L) and gently shaken for a few minutes. The degree of exchange of anionic dyes of solutions with different adsorption times was monitored by liquid-phase UV-vis spectroscopy based on typical absorption peaks of MB at 550 and 630 nm. As with the above methods, the anionic dyes MO and CR were tested experimentally. The characteristic peak of MO is at 460 nm, and the characteristic peak of CR is at 500 nm. In a similar way, we measured the UV-vis spectra of MBL and RhB ions. Additionally, the removal rate and concentration decays of organic dyes versus time were calculated from the time-dependent study. Moreover, the pseudo-first-order kinetic model and pseudo-second-order model kinetic model were used for kinetics data of organic dyes to be fitted in Table S1 and Figure S8.

**Calculation of Capacity.** Five milligrams of activated QUST-iPOP-1 was kept with 2.5 mL of the 5 mM oxo-anion or 60 mg L<sup>-1</sup> anionic organic dye solution for 24 h under stirring conditions. From the initial and final absorbance values of the oxo-anions or anionic organic dyes solutions, we calculated the storage capacity of QUST-iPOP-1 in 1 day using the following equation,

$$Q_t = \frac{(C_0 - C_t) \times V}{m} \quad (1)$$

where,  $Q_t$ ,  $C_0$ ,  $C_t$ ,  $V$ , and  $m$  are the capacity of the adsorbent, the initial concentration of the oxo-anions or anionic organic dyes solution, the

concentration of the solution at specific times, the volume of the solution, and the mass used for the adsorbent, respectively.

**Recyclability Test.** The samples (5 mg) after adsorption of anions were regenerated with a 5 M KCl (10 mL) solution for 24 h. The repeatability of regenerated materials was examined in 5 mL of 0.5 mM oxo-anionic solutions ( $MnO_4^-$ ,  $ReO_4^-$ , and  $Cr_2O_7^{2-}$ ) and 60 mg/L anionic dye solutions (MB, MO, and CR). The concentration of anionic solution was determined by UV-vis spectroscopy after 24 h of immersion. Each sample of this study was repeatedly tested three times.

In addition, the same approach was taken for the column where 5 M KCl was used to wash and regenerate the adsorbent.

## RESULTS AND DISCUSSION

As described in Figure 1, QUST-iPOP-1 was synthesized by a quaternization reaction between tri(4-imidazolylphenyl)amine (TIPA) and cyanuric chloride (CC) followed by the addition of benzyl bromide to confirm the complete reaction of the imidazole group in TIPA.<sup>78</sup> The chemical structure of QUST-iPOP-1 was clearly ascertained by solid-state <sup>13</sup>C NMR and FTIR spectra. As shown in Figure 2a, the disappearance of the

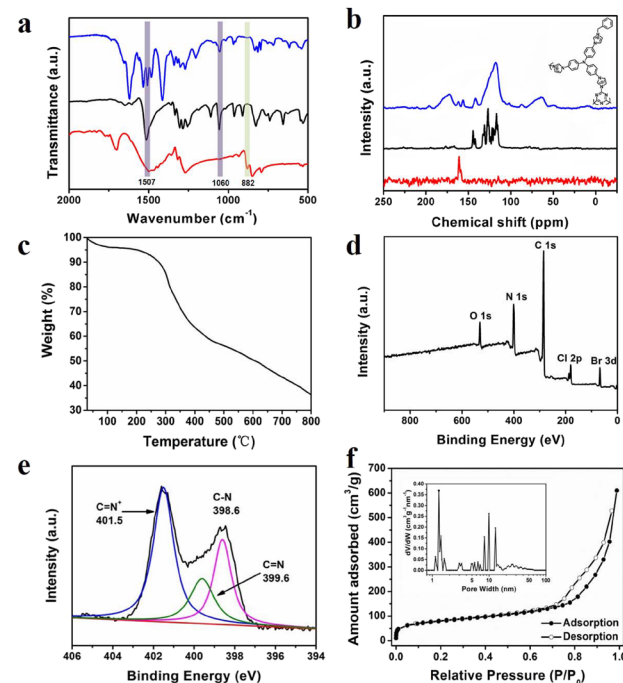


**Figure 2.** (a) FTIR spectrum of QUST-iPOP-1 (blue), TIPA (black), and CC (red). (b) Solid-state <sup>13</sup>C NMR spectrum of QUST-iPOP-1 (blue), TIPA (black), and CC (red). (c) TGA curve for QUST-iPOP-1. (d) XPS survey spectra of QUST-iPOP-1. (e) XPS spectra of N 1s for QUST-iPOP-1. (f) Nitrogen adsorption-desorption isotherm of QUST-iPOP-1. The inset is the pore size distribution profile obtained from the adsorption branch by the NLDFT method.

C–Cl bond stretching vibration at 882 cm<sup>-1</sup> indicates the complete reaction of cyanuric chloride. The peaks at 1507 and 1060 cm<sup>-1</sup> are assigned to the vibration of the imidazolium ring, further proving the successful formation of the ionic polymer.<sup>79</sup> The solid-state <sup>13</sup>C NMR spectrum of QUST-iPOP-1 (Figure 2b) revealed that the broad characteristic peaks that range from 100 to 147 ppm are ascribed to the carbon atoms on the TIPA unit and the benzene of benzyl bromide. The broad peaks in the region from 55 to 80 ppm correspond to the carbon atom of methylene from benzyl

bromide. Additionally, the characteristic peak at 170 ppm can be attributed to the carbon atoms of cyanuric chloride units.<sup>80</sup> As shown in Figure 2c, thermogravimetric data analysis showed that the stability of QUST-iPOP-1 can approach 300 °C. The weight loss before 100 °C corroborated the loss of guest molecules such as water molecules. XPS data analysis exhibited that the ionic polymer contained Cl<sup>-</sup> and Br<sup>-</sup>, demonstrating the successful synthesis of ionic polymers (Figure 2d). The XPS spectra of N 1s confirmed the existence of three N-containing functional groups (C=N<sup>+</sup>, C-N, and C≡N) in QUST-iPOP-1 (Figure 2e).

Nitrogen adsorption–desorption measurement was performed and used to analyze the porosity of QUST-iPOP-1. As shown in Figure 2f, QUST-iPOP-1 possesses a BET specific surface area of up to 274 m<sup>2</sup> g<sup>-1</sup> and a pore volume of up to 0.58 cm<sup>3</sup> g<sup>-1</sup> at  $P/P_0 = 0.95$ . The sorption isotherm belongs to a combination of type I and IV features on the basis of the IUPAC classification. The rapid adsorption of N<sub>2</sub> under  $P/P_0 < 0.01$  indicates the microporous structures within the polymer network. The obvious hysteresis between the adsorption and desorption isotherm reveals mesopores, while the sharp increase in the adsorbed amount of nitrogen after  $P/P_0 = 0.90$  indicates the existence of macropores. The pore size distribution profile obtained from the adsorption branch (Figure 2f) based on nonlocal density functional theory provides further evidence of the dominant existence of hierarchical pores in the polymer structure.

The morphology and porous structure were investigated by SEM and TEM. Both the SEM and TEM images (Figure 3a,b)

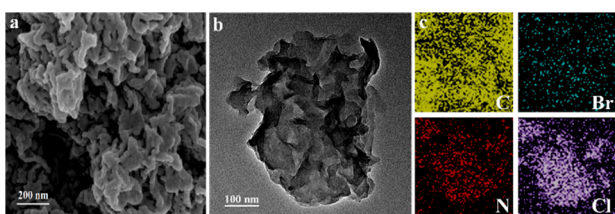


**Figure 3.** (a) SEM image of QUST-iPOP-1. (b) TEM image of QUST-iPOP-1. (c) Elemental mapping for C, N, Br, and Cl in QUST-iPOP-1.

show that QUST-iPOP-1 is amorphous. As shown in Figure 3c, the mapping data supported the presence of free Cl<sup>-</sup> and Br<sup>-</sup>. Powder X-ray diffraction further demonstrates the structure of the polymer, and PXRD data proves the amorphous nature of the material, which is similar to many other reported ionic polymer materials (Figure S1).<sup>81</sup> The electron diffraction test data (Figure S2) further proves that the material is an amorphous pure carbon material. The above data complement each other to fully confirm the successful synthesis of the polymers we designed. As shown in Figure S3, we compared the zeta potentials of the QUST-iPOP-1 and the mixture of the raw material at different pH levels and explored the effect of the quaternary amine group and pH on the surface charge. In the entire pH range, the zeta potentials of QUST-iPOP-1 are always higher than the potentials of the raw material mixture, which indicates that the formation of quaternary amine groups increases the surface potential of the material. This result shows that there probably exists a strong electrostatic adsorption between QUST-iPOP-1 and anions, which is consistent with the published data.<sup>82,83</sup> Since the zeta potential is more negative at higher pH values, the

adsorption of anions is expected to decrease due to electrostatic effects. Therefore, there is a positive correlation between the removal of anions and the zeta potential.

Based on the structural characteristics of the integrated polymer, we studied the adsorption of contaminated anions and dyes. Due to the presence of free Cl<sup>-</sup> and Br<sup>-</sup> ions in the pores of the polymer, it is more convenient for us to conduct ion adsorption studies. The compound is stable and insoluble in common aqueous and organic reagents, which opens up possibilities for our experiments. We first carried out adsorption experiments on Cr<sub>2</sub>O<sub>7</sub><sup>2-</sup> ions. As shown in Figure 4a, 2 mg of the compound was added to 4 mL of 0.5 mM Cr<sub>2</sub>O<sub>7</sub><sup>2-</sup> ion solution, and over time, we monitored the characteristic peaks at 265 and 365 nm by UV-vis spectroscopy. When the time reaches 60 min, the adsorption reaches a stable equilibrium, and the adsorption rate reaches 84.7% (Figure 4d). In order to explore the ability of the compound to adsorb radioactive TcO<sub>4</sub><sup>-</sup> ions, we chose the nonradioactive surrogates MnO<sub>4</sub><sup>-</sup> and ReO<sub>4</sub><sup>-</sup> instead. With regards to the adsorption effect of the compound on MnO<sub>4</sub><sup>-</sup> and ReO<sub>4</sub><sup>-</sup> ions, 2 mg of the compound was separately dispersed in a 0.5 mM potassium permanganate solution (4 mL) and a 0.5 mM ammonium perrhenate solution (4 mL). As shown in Figure 4b,c, over time, characteristic peaks at 525 nm ( $\lambda_{\text{max}}$  for MnO<sub>4</sub><sup>-</sup>) and 208 nm ( $\lambda_{\text{max}}$  for ReO<sub>4</sub><sup>-</sup>) were monitored by UV-vis spectroscopy. For MnO<sub>4</sub><sup>-</sup>, the absorption spectra decreased rapidly and the solution was decolorized within 8 min, and the adsorption rate is as high as 100%. As for the bigger size of ReO<sub>4</sub><sup>-</sup>, relatively slow kinetics were detected and the adsorption rate was 72.6% (Figure 4e,f). In order to simulate the actual environment to explore the ability of compounds to capture anions, we chose the main competitive ions Cl<sup>-</sup>, Br<sup>-</sup>, NO<sub>3</sub><sup>-</sup>, and SO<sub>4</sub><sup>2-</sup> in the wastewater for investigation. As shown Figure 4g–i, even in the presence of competing anions, the adsorption of the target anion is substantially unaffected, and the adsorption rate is basically close to 100%. This binary mixture study shows that the compound is highly efficient in capturing oxo-anions even in the presence of competing anions. As shown in Figure S13, taking MnO<sub>4</sub><sup>-</sup> as an example, the XPS data of the material after adsorption in the presence of competing anions shows that it has a very efficient selective adsorption effect on MnO<sub>4</sub><sup>-</sup>. So, we believe that the demonstrated excellent selectivity is due to the fact that the molecular space volume of the competing anion is much smaller than those of the target anion and the anion dye, so the pore size of the material has a greater restriction on the target anion, and the interaction between the material and the target anion is greater.

By virtue of such good absorbability of oxo-anions, we further explored its ability to adsorb anionic organic dyes. We selected three kinds of anionic dyes, MB, MO, and CR, and two kinds of cationic dyes for comparison, MLB and RhB. We prepared these five organic dye solutions at a concentration of 60 mg L<sup>-1</sup>, and took 6 mL of the above solution to add 2 mg of the compound to study its adsorption capacity. As shown in Figure 5a–c, the ionic polymer has an eventful adsorption effect on the anionic dyes. On the contrary, the cationic dyes were just slightly adsorbed by the compound (Figure 5d,e). As shown in Figure 5f, the adsorption rates of the compounds on the anionic dyes MB, MO, and CR were 88.2, 87.4, and 79.2%, respectively. The adsorption of the anionic organic dye further confirmed that the compound was a cationic backbone polymer and free Cl<sup>-</sup> and Br<sup>-</sup> existed in the pores. Figure S4

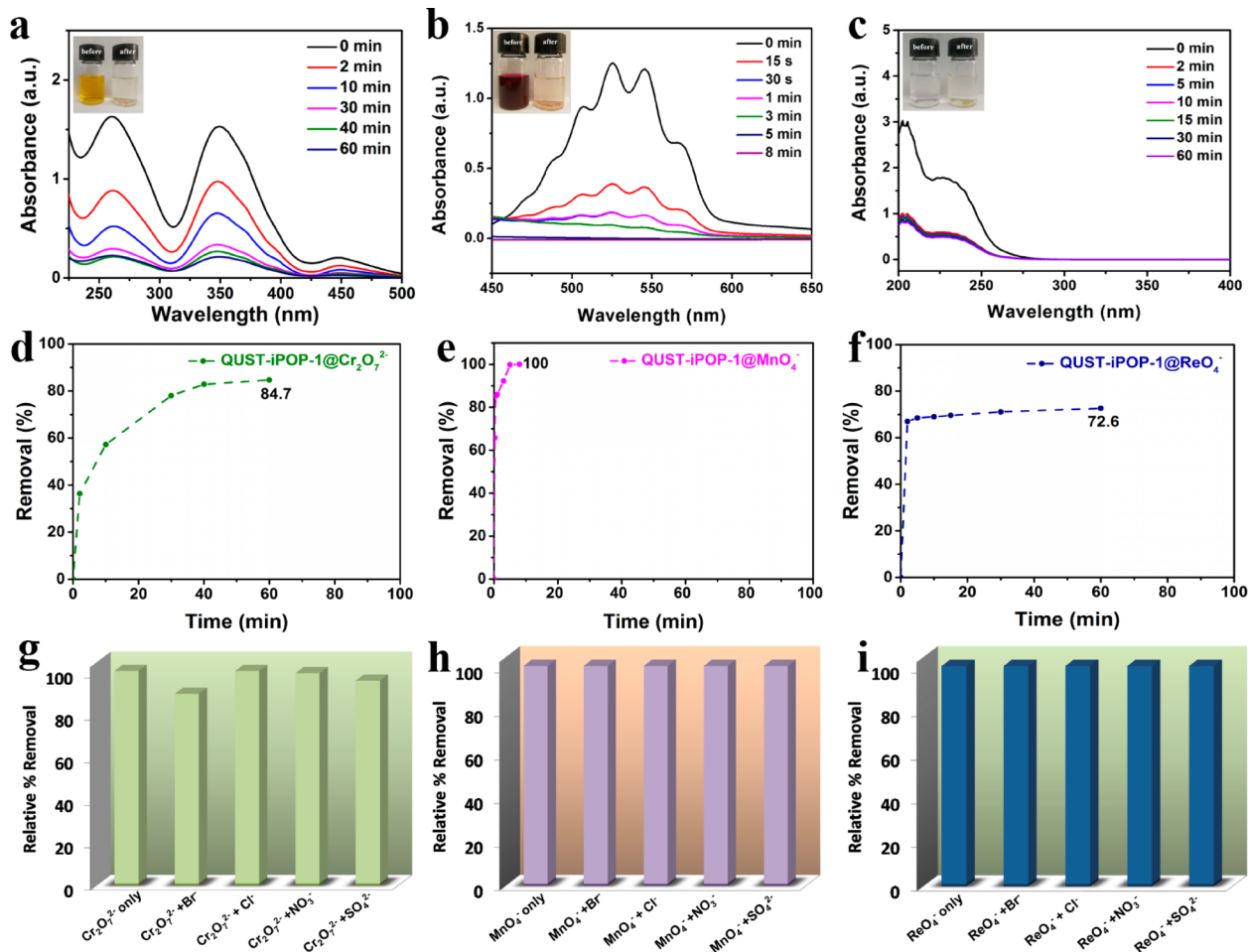


**Figure 4.** UV-vis spectroscopy in the presence of QUST-iPOP-1 at different time intervals for the water solution of (a) Cr<sub>2</sub>O<sub>7</sub><sup>2-</sup> ions, (b) MnO<sub>4</sub><sup>-</sup> ions, and (c) ReO<sub>4</sub><sup>-</sup> ions. Removal (in %) of (d) Cr<sub>2</sub>O<sub>7</sub><sup>2-</sup> ions, (e) MnO<sub>4</sub><sup>-</sup> ions, and (f) ReO<sub>4</sub><sup>-</sup> ions with QUST-iPOP-1 at different time intervals. The bar diagrams represent the removal efficiency of QUST-iPOP-1 in the presence of anions like Cl<sup>-</sup>, Br<sup>-</sup>, NO<sub>3</sub><sup>-</sup>, and SO<sub>4</sub><sup>2-</sup> for (g) Cr<sub>2</sub>O<sub>7</sub><sup>2-</sup> ions, (h) MnO<sub>4</sub><sup>-</sup> ions, and (i) ReO<sub>4</sub><sup>-</sup> ions.

shows the UV adsorption test of MnO<sub>4</sub><sup>-</sup> ions and methyl blue at 40 and 60 °C, respectively. It can be clearly seen from the figure that the higher the temperature, the faster the adsorption rate is. This may be due to the increase in temperature and the faster thermal movement of molecules, resulting in a faster ion exchange rate. In addition, we have tested the pH value of the solution before and after the adsorption (see Table S5), and we can see that the pH after adsorption has been significantly reduced. We believe that the Cl<sup>-</sup> and Br<sup>-</sup> ion exchanges lower the pH of the solution.

To further confirm the structural integrity of the polymer-adsorbed contaminated anions, we performed FTIR spectrum tests on the adsorbed polymer. As shown Figure S5a, the infrared characteristic peaks of the ionic polymer after adsorbing potassium dichromate ions appeared at 938 and 760 cm<sup>-1</sup>, demonstrating the successful adsorption of potassium dichromate ions. As shown Figure S5b,c, the infrared characteristic peaks of the polymer after adsorption of potassium permanganate and ammonium perrhenate appeared at 900 and 910 cm<sup>-1</sup>, respectively, which proved that potassium permanganate ions and ammonium perrhenate ions were successfully adsorbed. It was confirmed in the FTIR spectrum that the structure of the ionic polymer remained intact after absorbing the contaminating oxo-anions and anionic organic dyes (Figure S6).

In order to better understand the adsorption mechanism of the material and the change of the functional group on the material, we carried out the XPS test on the adsorption material. As shown in Figure 2e, a typical N 1s nuclear order spectrum of QUST-iPOP-1 shows the existence of three N-containing functional groups: C=N<sup>+</sup> (401.5 eV), C–N (398.6 eV), and C=N (399.6 eV).<sup>73</sup> As shown in Figure 6b,d,f–i, the binding energy of C=N<sup>+</sup> for the adsorbed material is differently higher than that for QUST-iPOP-1, which indicates that there is a strong electrostatic interaction between the positively charged cationic framework and the negatively charged oxyanions and anionic dyes. Additionally, according to the XPS test data in Figure 6a,c,e, we found that the corresponding elements Cr, Mn, and Re are obviously present in the material that adsorbs the corresponding oxygen-containing anions.

As shown in Figure S12, after 2 min of adsorption in the mixture solution of Cr<sub>2</sub>O<sub>7</sub><sup>2-</sup>, MnO<sub>4</sub><sup>-</sup>, and ReO<sub>4</sub><sup>-</sup>, QUST-iPOP-1 exhibited a faster adsorption rate for MnO<sub>4</sub><sup>-</sup> and ReO<sub>4</sub><sup>-</sup>, which may be due to the fact that Cr<sub>2</sub>O<sub>7</sub><sup>2-</sup> has two negative charges and a relatively large molecular space volume. Therefore, we believe that the hierarchical pores of this material may be more suitable for the exchange of oxygen-containing anions with a single negative charge and a relatively small molecular space volume. This further proves that the

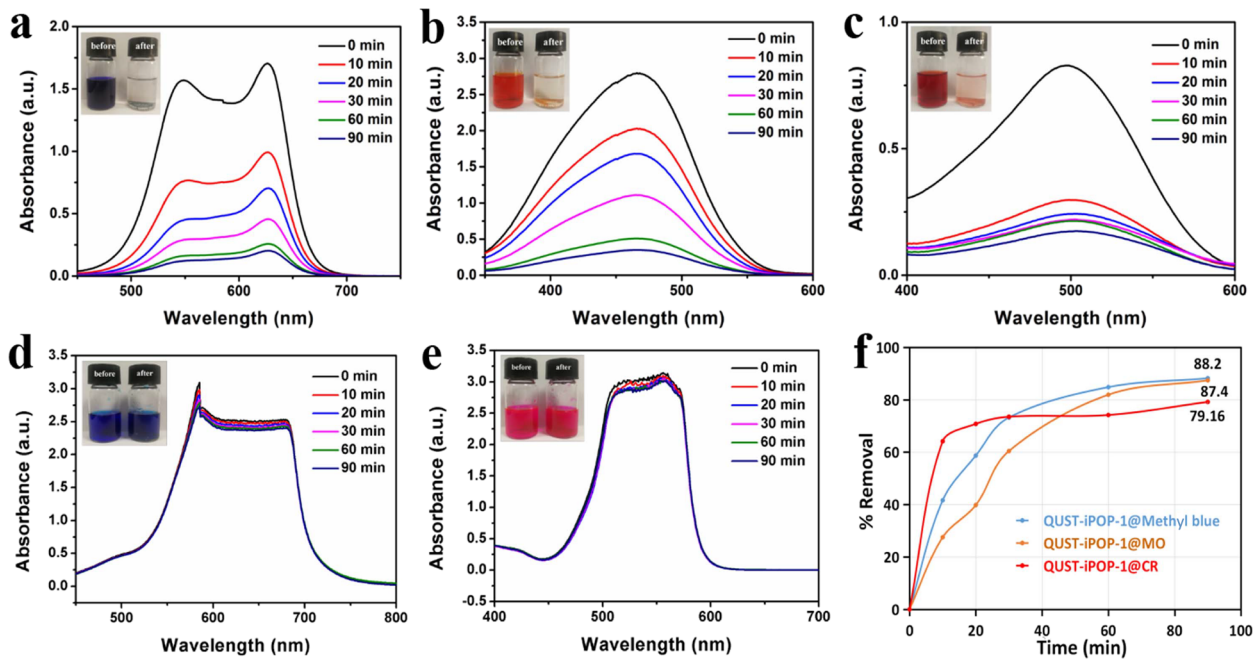


**Figure 5.** UV-vis spectroscopy in the presence of QUST-iPOP-1 at different time intervals for the water solution of anionic dyes (a) MB, (b) MO, and (c) CR and cationic dyes (d) MLB and (e) RhB. Removal (in %) of (f) MB, MO, and CR.

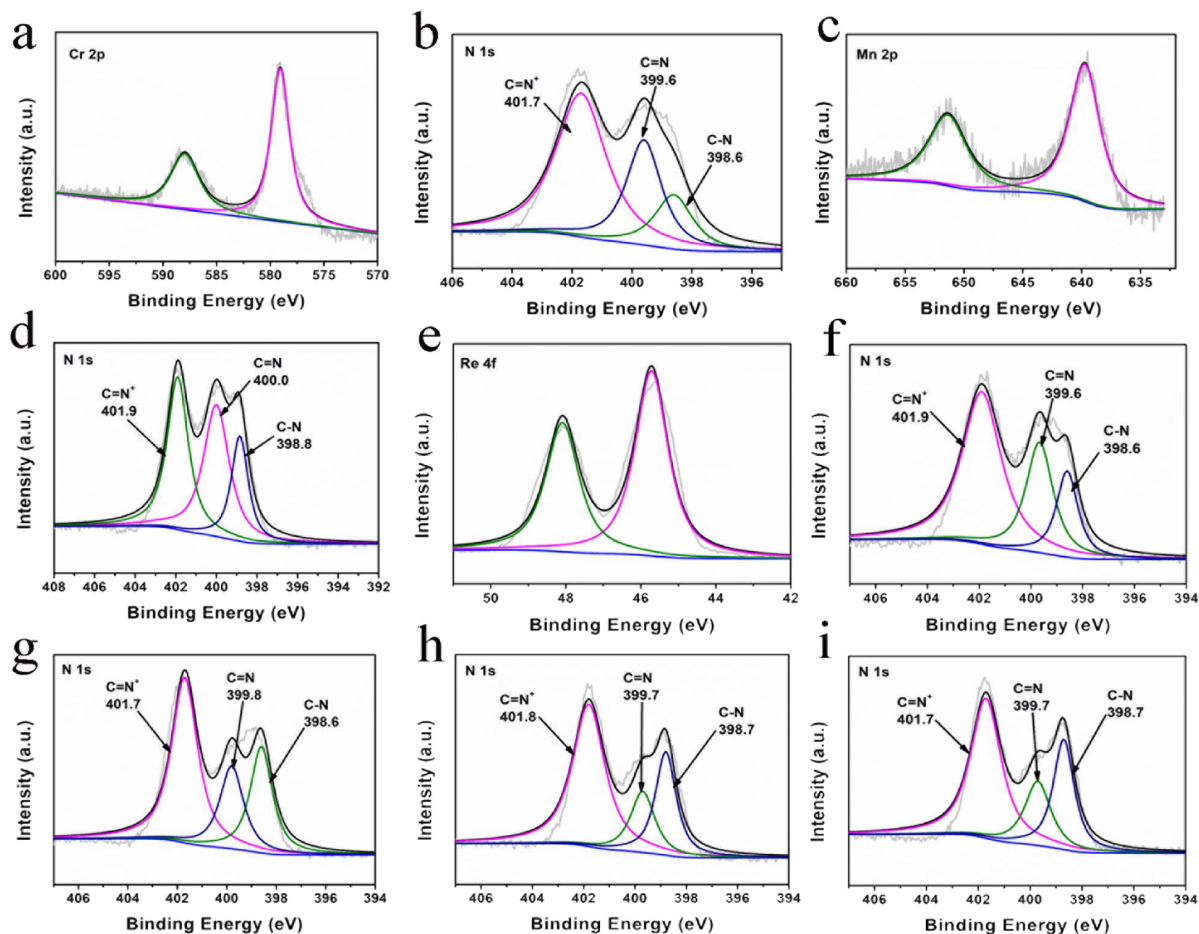


**Figure 6.** XPS spectra of (a) Cr 2p and (b) N 1s for QUST-iPOP-1-adsorbed  $\text{Cr}_2\text{O}_7^{2-}$ , (c) Mn 2p and (d) N 1s for QUST-iPOP-1-adsorbed  $\text{MnO}_4^-$ , (e) Re 4f and (f) N 1s for QUST-iPOP-1-adsorbed  $\text{ReO}_4^-$ , (g) N 1s for QUST-iPOP-1-adsorbed MB, (h) N 1s for QUST-iPOP-1-adsorbed MO, and (i) N 1s for QUST-iPOP-1-adsorbed CR.

adsorption mechanism of our material is caused by ion exchange, which relies on the electrostatic interaction between the cation framework and the anion.

In order to further study the adsorption mechanism, two different rate equations were used to study the kinetic process, named pseudo-first-order kinetic equation and pseudo-second-order kinetic equation. The pseudo-second-order kinetic model obtained a high correlation coefficient ( $R^2 > 0.99$ ), which indicates that the adsorption rate of anionic pollutant ions and dyes on QUST-iPOP-1 depends on the availability of active sites (Table S1). We constructed a Langmuir adsorption isotherm model to study the adsorption capacity of QUST-iPOP-1 to oxo-anions and anionic dyes pollutants. As shown in Figure S9, the results show that the Langmuir equation is in good agreement with the adsorption curve, indicating that the pollutants are adsorbed on the network surface in a single layer. After calculation, QUST-iPOP-1 exhibited an ultrahigh adsorption capacity for anionic dyes MB, CR, and oxo-anion  $\text{MnO}_4^-$ . As shown in Figure S9, the maximum adsorption capacities of MB, CR, and  $\text{MnO}_4^-$  were 1146.9, 1074.9, and 514.7 mg/g, respectively. Notably, the capacities of QUST-iPOP-1 for MB, CR, and  $\text{MnO}_4^-$  can be considered as one of the highest values in porous materials (Tables S3 and S4). Meanwhile, the maximum adsorption capacities of  $\text{Cr}_2\text{O}_7^{2-}$ ,  $\text{ReO}_4^-$ , and MO were 396.0, 441.6, and 300.0 mg/g, respectively, which were again some of the highest values in the reported well-performing compounds (Tables S2–S4). The maximum adsorption capacities exhibited by QUST-iPOP-1 are broadly higher than that of the general polymer for contaminated anions and organic dyes, which may be due to the wide pore size distribution and the strong forces from the cationic framework.

Furthermore, the renewable cycle test data show that no significant changes in the efficiency of the polymer was observed up to three cycles (Figure S10). Moreover, we designed and prepared chromatographic columns with compounds to separate polluting oxo-anions and anionic organic dyes in water (Figure S11). For  $\text{MnO}_4^-$  ions and MB as examples (1.0 mM stock solution), the eluates both undergo significant color changes, which is the result of being captured by QUST-iPOP-1 (Figure 7a,c). In addition, UV-vis studies indicated the absence of the  $\text{MnO}_4^-$  ions or MB in the eluent, which ascertained that the QUST-iPOP-1-based column is efficient to remove anionic pollutants (Figure 7b,d).

## CONCLUSIONS

In short, we successfully designed and constructed a cationic porous organic polymer QUST-iPOP-1 through the quaternization reaction. The rapid capture of anionic contaminants from water was demonstrated due to the presence of a special exchangeable  $\text{Cl}^-/\text{Br}^-$ -rich structure with high permanent porosity and wide pore size distribution. QUST-iPOP-1 showed high adsorption capacity and good recyclability and has significant selectivity even in the presence of large amounts of interfering anions like  $\text{Cl}^-$ ,  $\text{Br}^-$ ,  $\text{NO}_3^-$ ,  $\text{SO}_4^{2-}$ , etc. Rapid decolorization of the fuchsia-colored  $\text{MnO}_4^-$  and the blue-colored MB solution was observed owing to the effective removal of anionic pollutants from water in the presence of QUST-iPOP-1. These remarkable results indicate that this unique cationic porous organic network possesses dual capture capability of both oxo-anions and anionic organic dyes, which is not common in this field. This work opens up a new idea for

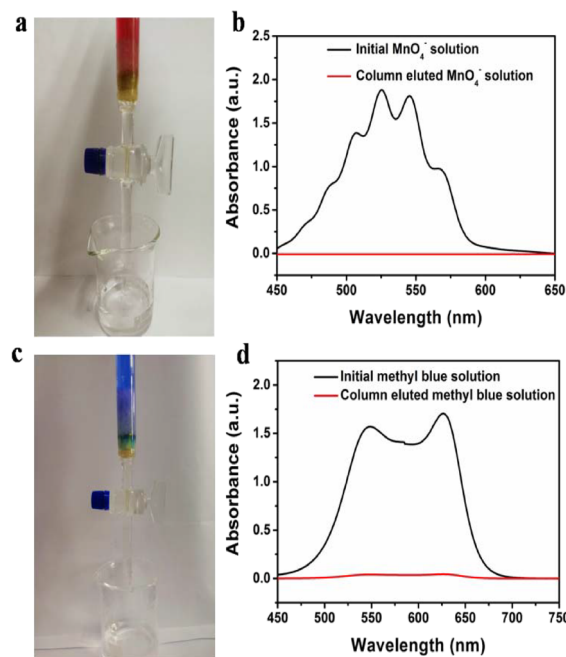


**Figure 7.** (a) Image and (b) UV-vis spectra of the  $\text{MnO}_4^-$  solution before and after passing through the compound-loaded packed column. (c) Image and (d) UV-vis spectra of the methyl blue solution before and after passing through the compound-loaded packed column.

the construction of excellent adsorption materials at the molecular level.

## ASSOCIATED CONTENT

### SI Supporting Information

The Supporting Information is available free of charge at <https://pubs.acs.org/doi/10.1021/acsmi.1c10464>.

PXRD data of QUST-iPOP-1; FTIR spectrum of QUST-iPOP-1-adsorbed  $\text{Cr}_2\text{O}_7^{2-}$ ,  $\text{MnO}_4^-$ , and  $\text{ReO}_4^-$  and FTIR spectrum of QUST-iPOP-1-adsorbed MB, MO, CR, MLB, and RhB; pseudo-first-order model of  $\text{K}_2\text{Cr}_2\text{O}_7$ ,  $\text{KMnO}_4$ , and  $\text{NH}_4\text{ReO}_4$  and pseudo-second-order model of  $0.5 \text{ mmol L}^{-1}$   $\text{K}_2\text{Cr}_2\text{O}_7$ ,  $\text{KMnO}_4$ , and  $\text{NH}_4\text{ReO}_4$ ; pseudo-first-order model of MB, MO, and CR and pseudo-second-order model of  $60 \text{ mg L}^{-1}$  MB, MO, and CR; equilibrium adsorption isotherms of  $\text{K}_2\text{Cr}_2\text{O}_7$ ,  $\text{KMnO}_4$ ,  $\text{NH}_4\text{ReO}_4$ , MB, MO, and CR onto QUST-iPOP-1 with Langmuir fits; recyclability test of the compound; representation of compound-loaded columns used for column chromatography to separate oxygen anions; table data of the parameters of the different adsorption kinetic models extracted from experimental adsorption data for QUST-iPOP-1; adsorption capacity of  $\text{Cr}_2\text{O}_7^{2-}$ , adsorption capacity of  $\text{MnO}_4^-$  and  $\text{ReO}_4^-$ , and adsorption capacity of MB, MO, and CR; and data of references (PDF)

## AUTHOR INFORMATION

### Corresponding Authors

Kang Liu – Key Laboratory of Eco-chemical Engineering, Key Laboratory of Optic-electric Sensing and Analytical Chemistry of Life Science, Taishan Scholar Advantage and Characteristic Discipline Team of Eco Chemical Process and

Technology, College of Chemistry and Molecular Engineering, Qingdao University of Science and Technology, Qingdao 266042, P. R. China; [orcid.org/0000-0002-3436-7850](https://orcid.org/0000-0002-3436-7850); Email: liukang82@126.com

**Dingxuan Ma** – Key Laboratory of Eco-chemical Engineering, Key Laboratory of Optic-electric Sensing and Analytical Chemistry of Life Science, Taishan Scholar Advantage and Characteristic Discipline Team of Eco Chemical Process and Technology, College of Chemistry and Molecular Engineering, Qingdao University of Science and Technology, Qingdao 266042, P. R. China; [orcid.org/0000-0002-0848-5167](https://orcid.org/0000-0002-0848-5167); Email: madingxuan640@126.com

## Authors

**Shaoshao Jiao** – Key Laboratory of Eco-chemical Engineering, Key Laboratory of Optic-electric Sensing and Analytical Chemistry of Life Science, Taishan Scholar Advantage and Characteristic Discipline Team of Eco Chemical Process and Technology, College of Chemistry and Molecular Engineering, Qingdao University of Science and Technology, Qingdao 266042, P. R. China

**Liming Deng** – Jiangsu Key Laboratory of Materials and Technology for Energy Conversion, College of Materials Science and Technology, Nanjing University of Aeronautics and Astronautics, Nanjing 210016, P. R. China

**Xinghao Zhang** – Key Laboratory of Eco-chemical Engineering, Key Laboratory of Optic-electric Sensing and Analytical Chemistry of Life Science, Taishan Scholar Advantage and Characteristic Discipline Team of Eco Chemical Process and Technology, College of Chemistry and Molecular Engineering, Qingdao University of Science and Technology, Qingdao 266042, P. R. China

**Yaowen Zhang** – Key Laboratory of Eco-chemical Engineering, Key Laboratory of Optic-electric Sensing and Analytical Chemistry of Life Science, Taishan Scholar Advantage and Characteristic Discipline Team of Eco Chemical Process and Technology, College of Chemistry and Molecular Engineering, Qingdao University of Science and Technology, Qingdao 266042, P. R. China

**Shaoxiang Li** – Shandong Engineering Research Center for Marine Environment Corrosion and Safety Protection, College of Environment and Safety Engineering, Qingdao University of Science and Technology, Qingdao 266042, P. R. China

**Lei Wang** – Key Laboratory of Eco-chemical Engineering, Key Laboratory of Optic-electric Sensing and Analytical Chemistry of Life Science, Taishan Scholar Advantage and Characteristic Discipline Team of Eco Chemical Process and Technology, College of Chemistry and Molecular Engineering and Shandong Engineering Research Center for Marine Environment Corrosion and Safety Protection, College of Environment and Safety Engineering, Qingdao University of Science and Technology, Qingdao 266042, P. R. China; [orcid.org/0000-0001-7275-4846](https://orcid.org/0000-0001-7275-4846)

Complete contact information is available at:  
<https://pubs.acs.org/10.1021/acsami.1c10464>

## Author Contributions

The manuscript was written through contributions of all authors. All authors have given approval to the final version of the manuscript.

## Notes

The authors declare no competing financial interest.

## ACKNOWLEDGMENTS

This work was supported by the Natural Science Foundation of Shandong Province, China (No. ZR2020QB035), the National Natural Science Foundation of China (nos. 21601103, 51572136, and 51772162), and the Taishan Scholars Program.

## REFERENCES

- (1) Oliver, S. R. J. Cationic Inorganic Materials for Anionic Pollutant Trapping and Catalysis. *Chem. Soc. Rev.* **2009**, *38*, 1868–1881.
- (2) Schwarzenbach, R. P.; Egli, T.; Hofstetter, T. B.; von Gunten, U.; Wehrli, B. Global Water Pollution and Human Health. *Annu. Rev. Environ. Resour.* **2010**, *35*, 109–136.
- (3) Watharkar, A. D.; Kadam, S. K.; Khadare, R. V.; Kolekar, P. D.; Jeon, B. H.; Jadhav, J. P.; Govindwar, S. P. *Asparagus Densiflorus* in a Vertical Subsurface Flow Phytoreactor for Treatment of Real Textile Effluent: A Lab to Land Approach for *In Situ* Soil Remediation. *Ecotoxicol. Environ. Saf.* **2018**, *161*, 70–77.
- (4) Keith, L. H.; Tellier, W. A. Priority Pollutants: I. A Perspective View. *Environ. Sci. Technol.* **1979**, *13*, 416–423.
- (5) Costa, M.; Klein, C. B. Toxicity and Carcinogenicity of Chromium Compounds in Humans. *Crit. Rev. Toxicol.* **2006**, *36*, 155–163.
- (6) von Burg, R.; Liu, D. Chromium and Hexavalent Chromium. *J. Appl. Toxicol.* **1993**, *13*, 225–230.
- (7) Chowdhury, A.; Kumar, S.; Khan, A. A.; Hussain, S. Selective Removal of Anionic Dyes with Exceptionally High Adsorption Capacity and Removal of Dichromate ( $\text{Cr}_2\text{O}_7^{2-}$ ) Anion Using Ni-Co-S/CTAB Nanocomposites and Its Adsorption Mechanism. *J. Hazard. Mater.* **2020**, *385*, 121602–121616.
- (8) Westerhoff, P.; Zimmerman, J. B.; Field, J.; Lowry, G. Making Waves. *Environ. Sci. Technol.* **2020**, *54*, 6449–6450.
- (9) Banerjee, D.; Kim, D.; Schweiger, M. J.; Kruger, A. A.; Thallapally, P. K. Removal of  $\text{TcO}_4^-$  Ions from Solution: Materials and Future Outlook. *Chem. Soc. Rev.* **2016**, *45*, 2724–2739.
- (10) Lee, M.-S.; Um, W.; Wang, G.; Kruger, A. A.; Lukens, W. W.; Rousseau, R. V.; Glezakou, V.-A. Impeding  $^{99}\text{Tc}(\text{IV})$  Mobility in Novel Waste Forms. *Nat. Commun.* **2016**, *7*, 12067–12073.
- (11) Smith, F. N.; Taylor, C. D.; Um, W.; Kruger, A. A. Technetium Incorporation into Goethite ( $\alpha\text{-FeOOH}$ ): An Atomic-Scale Investigation. *Environ. Sci. Technol.* **2015**, *49*, 13699–13707.
- (12) Gupta, V. K.; Suhas. Application of low-cost adsorbents for dye removal – A review. *J. Environ. Manage.* **2009**, *90*, 2313–2342.
- (13) Rafatullah, M.; Sulaiman, O.; Hashim, R.; Ahmad, A. Adsorption of Methylene Blue on Low-Cost Adsorbents: A Review. *J. Hazard. Mater.* **2010**, *177*, 70–80.
- (14) Yagub, M. T.; Sen, T. K.; Afrose, S.; Ang, H. M. Dye and Its Removal from Aqueous Solution by Adsorption: A Review. *Adv. Colloid Interface Sci.* **2014**, *209*, 172–184.
- (15) Brillas, E.; Martínez-Huitle, C. A. Decontamination of Wastewaters Containing Synthetic Organic Dyes by Electrochemical Methods. An Updated Review. *Appl. Catal., B* **2015**, *166–167*, 603–643.
- (16) Cardoso, J. C.; Bessegato, G. G.; Zanoni, M. V. B. Efficiency Comparison of Ozonation, Photolysis, Photocatalysis and Photoelectrocatalysis Methods in Real Textile Wastewater Decolorization. *Water Res.* **2016**, *98*, 39–46.
- (17) Fu, F.; Wang, Q. Removal of Heavy Metal Ions from Wastewaters: A Review. *J. Environ. Manage.* **2011**, *92*, 407–418.
- (18) Barakat, M. A. New Trends in Removing Heavy Metals from Industrial Wastewater. *Arab. J. Chem.* **2011**, *4*, 361–377.
- (19) Sirtori, C.; Zapata, A.; Oller, I.; Gernjak, W.; Agüera, A.; Malato, S. Decontamination Industrial Pharmaceutical Wastewater by Combining Solar Photo-Fenton and Biological Treatment. *Water Res.* **2009**, *43*, 661–668.
- (20) Abdel-Raouf, N.; Al-Homaidan, A. A.; Ibraheem, I. B. M. Microalgae and Wastewater Treatment. *Saudi J. Biol. Sci.* **2012**, *19*, 257–275.

- (21) Yin, J.; Deng, B. Polymer-Matrix Nanocomposite Membranes for Water Treatment. *J. Membr. Sci.* **2015**, *479*, 256–275.
- (22) Fane, A. G.; Wang, R.; Hu, M. X. Synthetic Membranes for Water Purification: Status and Future. *Angew. Chem., Int. Ed.* **2015**, *54*, 3368–3386.
- (23) Luo, Y.; Guo, W.; Ngo, H. H.; Nghiem, L. D.; Hai, F. I.; Zhang, J.; Liang, S.; Wang, X. C. A Review on the Occurrence of Micropollutants in the Aquatic Environment and Their Fate and Removal during Wastewater Treatment. *Sci. Total Environ.* **2014**, *473-474*, 619–641.
- (24) Deng, S.-Q.; Mo, X.-J.; Zheng, S.-R.; Jin, X.; Gao, Y.; Cai, S.-L.; Fan, J.; Zhang, W.-G. Hydrolytically Stable Nanotubular Cationic Metal–Organic Framework for Rapid and Efficient Removal of Toxic Oxo-Anions and Dyes from Water. *Inorg. Chem.* **2019**, *58*, 2899–2909.
- (25) Boyer, T. H.; Singer, P. C. Stoichiometry of Removal of Natural Organic Matter by Ion Exchange. *Environ. Sci. Technol.* **2008**, *42*, 608–613.
- (26) Gammelgaard, B.; Liao, Y.-p.; Jøns, O. Improvement on Simultaneous Determination of Chromium Species in Aqueous Solution by Ion Chromatography and Chemiluminescence Detection. *Anal. Chim. Acta* **1997**, *354*, 107–113.
- (27) Wen, B.; Shan, X.-Q.; Lian, J. Separation of Cr(III) and Cr(VI) in River and Reservoir Water with 8-Hydroxyquinoline Immobilized Polyacrylonitrile Fiber for Determination by Inductively Coupled Plasma Mass Spectrometry. *Talanta* **2002**, *56*, 681–687.
- (28) Ma, J.; Yu, F.; Zhou, L.; Jin, L.; Yang, M.; Luan, J.; Tang, Y.; Fan, H.; Yuan, Z.; Chen, J. Enhanced Adsorptive Removal of Methyl Orange and Methylene Blue from Aqueous Solution by Alkali-Activated Multiwalled Carbon Nanotubes. *ACS Appl. Mater. Interfaces* **2012**, *4*, 5749–5760.
- (29) Ghosh, R.; Sahu, A.; Pushpavanam, S. Removal of Trace Hexavalent Chromium from Aqueous Solutions by Ion Foam Fractionation. *J. Hazard. Mater.* **2019**, *367*, 589–598.
- (30) Li, J.; Dai, X.; Zhu, L.; Xu, C.; Zhang, D.; Silver, M. A.; Li, P.; Chen, L.; Li, Y.; Zuo, D.; Zhang, H.; Xiao, C.; Chen, J.; Diwu, J.; Farha, O. K.; Albrecht-Schmitt, T. E.; Chai, Z.; Wang, S.  $^{99}\text{TcO}_4^-$  Remediation by a Cationic Polymeric Network. *Nat. Commun.* **2018**, *9*, 3007–3018.
- (31) Sheng, D.; Zhu, L.; Xu, C.; Xiao, C.; Wang, Y.; Wang, Y.; Chen, L.; Diwu, J.; Chen, J.; Chai, Z.; Albrecht-Schmitt, T. E.; Wang, S. Efficient and Selective Uptake of  $\text{TcO}_4^-$  by a Cationic Metal–Organic Framework Material with Open  $\text{Ag}^+$  Sites. *Environ. Sci. Technol.* **2017**, *51*, 3471–3479.
- (32) Ibrahim, Y.; Naddeo, V.; Banat, F.; Hasan, S. W. Preparation of Novel Polyvinylidene Fluoride (PVDF)-Tin(IV) Oxide ( $\text{SnO}_2$ ) Ion Exchange Mixed Matrix Membranes for the Removal of Heavy Metals from Aqueous Solutions. *Sep. Purif. Technol.* **2020**, *250*, 117250–117265.
- (33) Zhang, X.; Niu, J.; Hao, X.; Wang, Z.; Guan, G.; Abudula, A. A Novel Electrochemically Switched Ion Exchange System for Phenol Recovery and Regeneration of NaOH from Sodium Phenolate Wastewater. *Sep. Purif. Technol.* **2020**, *248*, 117125–117134.
- (34) Liu, Z.-W.; Han, B.-H. Evaluation of an Imidazolium-Based Porous Organic Polymer as Radioactive Waste Scavenger. *Environ. Sci. Technol.* **2019**, *54*, 216–224.
- (35) Khan, N. A.; Hasan, Z.; Jhung, S. H. Adsorptive Removal of Hazardous Materials Using Metal-Organic Frameworks (MOFs): A Review. *J. Hazard. Mater.* **2013**, *244–245*, 444–456.
- (36) Gupta, V. K.; Saleh, T. A. Sorption of Pollutants by Porous Carbon, Carbon Nanotubes and Fullerene- An Overview. *Environ. Sci. Pollut. Res.* **2013**, *20*, 2828–2843.
- (37) Wang, S.; Peng, Y. Natural Zeolites as Effective Adsorbents in Water and Wastewater Treatment. *Chem. Eng. J.* **2010**, *156*, 11–24.
- (38) Wang, J.; Zheng, S.; Shao, Y.; Liu, J.; Xu, Z.; Zhu, D. Amino-Functionalized  $\text{Fe}_3\text{O}_4@\text{SiO}_2$  Core–Shell Magnetic Nanomaterial as a Novel Adsorbent for Aqueous Heavy Metals Removal. *J. Colloid Interface Sci.* **2010**, *349*, 293–299.
- (39) Taylor, D.; Dalgarno, S. J.; Xu, Z.; Vilela, F. Conjugated Porous Polymers: Incredibly Versatile Materials with Far-Reaching Applications. *Chem. Soc. Rev.* **2020**, *49*, 3981–4042.
- (40) Liu, M.; Guo, L.; Jin, S.; Tan, B. Covalent Triazine Frameworks: Synthesis and Applications. *J. Mater. Chem. A* **2019**, *7*, 5153–5172.
- (41) McKeown, N. B. The Synthesis of Polymers of Intrinsic Microporosity (PIMs). *Sci. China Chem.* **2017**, *60*, 1023–1032.
- (42) Chen, D.; Liu, C.; Tang, J.; Luo, L.; Yu, G. Fluorescent Porous Organic Polymers. *Polym. Chem.* **2019**, *10*, 1168–1181.
- (43) Graetz, J. New Approaches to Hydrogen Storage. *Chem. Soc. Rev.* **2009**, *38*, 73–82.
- (44) Makal, T. A.; Li, J.-R.; Lu, W.; Zhou, H.-C. Methane Storage in Advanced Porous Materials. *Chem. Soc. Rev.* **2012**, *41*, 7761–7779.
- (45) Dawson, R.; Adams, D. J.; Cooper, A. I. Chemical Tuning of  $\text{CO}_2$  Sorption in Robust Nanoporous Organic Polymers. *Chem. Sci.* **2011**, *2*, 1173–1177.
- (46) Yang, Z.; Zhang, Y.; Wang, X.; Tian, Z.; Yang, W.; Graham, N. J. D. Efficient Adsorption of Four Phenolic Compounds Using a Robust Nanocomposite Fabricated by Confining 2D Porous Organic Polymers in 3D Anion Exchangers. *Chem. Eng. J.* **2020**, *396*, 125296–125307.
- (47) Che, S.; Pang, J.; Kalin, A. J.; Wang, C.; Ji, X.; Lee, J.; Cole, D.; Li, J.-L.; Tu, X.; Zhang, Q.; Zhou, H.-C.; Fang, L. Rigid Ladder-Type Porous Polymer Networks for Entropically Favorable Gas Adsorption. *ACS Mater. Lett.* **2020**, *2*, 49–54.
- (48) Lee, H.; Kim, H.; Choi, T. J.; Park, H. W.; Chang, J. Y. Preparation of a Microporous Organic Polymer by the Thiol-yne Addition Reaction and Formation of Au Nanoparticles Inside the Polymer. *Chem. Commun.* **2015**, *51*, 9805–9808.
- (49) Li, L.; Zhao, H.; Wang, R. Tailorable Synthesis of Porous Organic Polymers Decorating Ultrafine Palladium Nanoparticles for Hydrogenation of Olefins. *ACS Catal.* **2015**, *5*, 948–955.
- (50) Lu, Y.; Chang, Z.; Zhang, S.; Wang, S.; Chen, Q.; Feng, L.; Sui, Z. Porous Organic Polymers Containing Zinc Porphyrin and Phosphonium Bromide as Bifunctional Catalysts for Conversion of Carbon Dioxide. *J. Mater. Sci.* **2020**, *55*, 11856–11869.
- (51) Ravi, S.; Choi, Y.; Choe, J. K. Achieving Effective Fructose-to-5-Hydroxymethylfurfural Conversion via Facile Synthesis of Large Surface Phosphate-Functionalized Porous Organic Polymers. *Appl. Catal., B* **2020**, *271*, 118942–118954.
- (52) Puthiaraj, P.; Yu, K.; Baeck, S.-H.; Ahn, W.-S. Cascade Knoevenagel Condensation-Chemoselective Transfer Hydrogenation Catalyzed by Pd Nanoparticles Stabilized on Amine-Functionalized Aromatic Porous Polymer. *Catal. Today* **2020**, *352*, 298–307.
- (53) Chakraborty, J.; Nath, I.; Song, S.; Kao, C.-M.; Verpoort, F. Synergistic Performance of a Sub-Nanoscopic Cobalt and Imidazole Grafted Porous Organic Polymer for  $\text{CO}_2$  Fixation to Cyclic Carbonates under Ambient Pressure without a Co-Catalyst. *J. Mater. Chem. A* **2020**, *8*, 13916–13920.
- (54) Zhang, K.; Kopetzki, D.; Seeger, P. H.; Antonietti, M.; Vilela, F. Surface Area Control and Photocatalytic Activity of Conjugated Microporous Poly(benzothiadiazole) Networks. *Angew. Chem., Int. Ed.* **2013**, *52*, 1432–1436.
- (55) Schwab, M. G.; Hamburger, M.; Feng, X.; Shu, J.; Spiess, H. W.; Wang, X.; Antonietti, M.; Müllen, K. Photocatalytic Hydrogen Evolution Through Fully Conjugated Poly(azomethine) Networks. *Chem. Commun.* **2010**, *46*, 8932–8934.
- (56) Chen, L.; Honsho, Y.; Seki, S.; Jiang, D. Light-Harvesting Conjugated Microporous Polymers: Rapid and Highly Efficient Flow of Light Energy with a Porous Polyphenylene Framework as Antenna. *J. Am. Chem. Soc.* **2010**, *132*, 6742–6748.
- (57) Liu, X.; Liu, C.-F.; Lai, W.-Y.; Huang, W. Porous Organic Polymers as Promising Electrode Materials for Energy Storage Devices. *Adv. Mater. Technol.* **2020**, *10*, 2000154–2000174.
- (58) Sapchenko, S. A.; Samsonenko, D. G.; Dybtsev, D. N.; Melgunov, M. S.; Fedin, V. P. Microporous Sensor: Gas Sorption, Guest Exchange and Guest-Dependant Luminescence of Metal–Organic Framework. *Dalton Trans.* **2011**, *40*, 2196–2203.

- (59) Zhang, H.; Ma, J.; Chen, D.; Zhou, J.; Zhang, S.; Shi, W.; Cheng, P. Microporous Heterometal–Organic Framework as a Sensor for BTEX with High Selectivity. *J. Mater. Chem. A* **2014**, *2*, 20450–20453.
- (60) Florea, A.; Guo, Z. Z.; Cristea, C.; Bessueille, F.; Vocanson, F.; Goutaland, F.; Dzyadevych, S.; Sandulescu, R.; Jaffrezic-Renault, N. Anticancer Drug Detection Using a Highly Sensitive Molecularly Imprinted Electrochemical Sensor Based on an Electropolymerized Microporous Metal Organic Framework. *Talanta* **2015**, *138*, 71–76.
- (61) Li, Y.; Fang, Y.; Gao, W.; Guo, X.; Zhang, X. Porphyrin-Based Porous Organic Polymer as Peroxidase Mimics for Sulfide-Ion Colorimetric Sensing. *ACS Sustainable Chem. Eng.* **2020**, *8*, 10870–10880.
- (62) He, L.; Liu, S.; Chen, L.; Dai, X.; Li, J.; Zhang, M.; Ma, F.; Zhang, C.; Yang, Z.; Zhou, R.; Chai, Z.; Wang, S. Mechanism Unravelling for Ultrafast and Selective  $^{99}\text{TcO}_4^-$  Uptake by a Radiation-Resistant Cationic Covalent Organic Framework: a Combined Radiological Experiment and Molecular Dynamics Simulation Study. *Chem. Sci.* **2019**, *10*, 4293–4305.
- (63) Li, Y.; Yang, Z.; Wang, Y.; Bai, Z.; Zheng, T.; Dai, X.; Liu, S.; Gui, D.; Liu, W.; Chen, M.; Chen, L.; Diwu, J.; Zhu, L.; Zhou, R.; Chai, Z.; Albrecht-Schmitt, T. E.; Wang, S. A Mesoporous Cationic Thorium-Organic Framework That Rapidly Traps Anionic Persistent Organic Pollutants. *Nat. Commun.* **2017**, *8*, 1354–1365.
- (64) Buyukcakir, O.; Je, S. H.; Talapaneni, S. N.; Kim, D.; Coskun, A. Charged Covalent Triazine Frameworks for  $\text{CO}_2$  Capture and Conversion. *ACS Appl. Mater. Interfaces* **2017**, *9*, 7209–7216.
- (65) Yu, S.-B.; Lyu, H.; Tian, J.; Wang, H.; Zhang, D.-W.; Liu, Y.; Li, Z.-T. A Polycationic Covalent Organic Framework: a Robust Adsorbent for Anionic Dye Pollutants. *Polym. Chem.* **2016**, *7*, 3392–3397.
- (66) Ong, W. S. Y.; Smaldone, R. A.; Dodani, S. C. A Neutral Porous Organic Polymer Host for the Recognition of Anionic Dyes in Water. *Chem. Sci.* **2020**, *11*, 7716–7721.
- (67) Liu, Z.-W.; Han, B.-H. Ionic Porous Organic Polymers for  $\text{CO}_2$  Capture and Conversion. *Curr. Opin. Green Sustainbale. Chem.* **2019**, *16*, 20–25.
- (68) Huang, L.; He, M.; Chen, B.; Cheng, Q.; Hu, B. Facile Green Synthesis of Magnetic Porous Organic Polymers for Rapid Removal and Separation of Methylene Blue. *ACS Sustainable Chem. Eng.* **2017**, *5*, 4050–4055.
- (69) Shen, J.; Chai, W.; Wang, K.; Zhang, F. Efficient Removal of Anionic Radioactive Pollutant from Water Using Ordered Urea-Functionalized Mesoporous Polymeric Nanoparticle. *ACS Appl. Mater. Interfaces* **2017**, *9*, 22440–22448.
- (70) Shen, X.; Ma, S.; Xia, H.; Shi, Z.; Mu, Y.; Liu, X. Cationic Porous Organic Polymers as an Excellent Platform for Highly Efficient Removal of Pollutants from Water. *J. Mater. Chem. A* **2018**, *6*, 20653–20658.
- (71) Su, Y.; Wang, Y.; Li, X.; Li, X.; Wang, R. Imidazolium-Based Porous Organic Polymers: Anion Exchange-Driven Capture and Luminescent Probe of  $\text{Cr}_2\text{O}_7^{2-}$ . *ACS Appl. Mater. Interfaces* **2016**, *8*, 18904–18911.
- (72) Da, H.-J.; Yang, C.-X.; Yan, X.-P. Cationic Covalent Organic Nanosheets for Rapid and Selective Capture of Perrhenate: An Analogue of Radioactive Pertechnetate from Aqueous Solution. *Environ. Sci. Technol.* **2019**, *53*, 5212–5220.
- (73) Ding, M.; Chen, L.; Xu, Y.; Chen, B.; Ding, J.; Wu, R.; Huang, C.; He, Y.; Jin, Y.; Xia, C. Efficient Capture of Tc/Re(VII, IV) by a Viologen-Based Organic Polymer Containing Tetraaza Macrocycles. *Chem. Eng. J.* **2020**, *380*, 122581–122592.
- (74) Liu, Z.-W.; Cao, C.-X.; Han, B.-H. A Cationic Porous Organic Polymer for High-Capacity, Fast, and Selective Capture of Anionic Pollutants. *J. Hazard. Mater.* **2019**, *367*, 348–355.
- (75) Mitra, S.; Kandambeth, S.; Biswal, B. P.; Khayum, M. A.; Choudhury, C. K.; Mehta, M.; Kaur, G.; Banerjee, S.; Prabhune, A.; Verma, S.; Roy, S.; Kharul, U. K.; Banerjee, R. Self-Exfoliated Guanidinium-Based Ionic Covalent Organic Nanosheets (iCONs). *J. Am. Chem. Soc.* **2016**, *138*, 2823–2828.
- (76) Li, Z.; Li, H.; Guan, X.; Tang, J.; Yusran, Y.; Li, Z.; Xue, M.; Fang, Q.; Yan, Y.; Valtchev, V.; Qiu, S. Three-Dimensional Ionic Covalent Organic Frameworks for Rapid, Reversible, and Selective Ion Exchange. *J. Am. Chem. Soc.* **2017**, *139*, 17771–17774.
- (77) Yao, X.-Q.; Cao, D.; Hu, J.-S.; Li, Y.-Z.; Guo, Z.-J.; Zheng, H.-G. Chiral and Porous Coordination Polymers Based on an N-Centered Triangular Rigid Ligand. *Cryst. Growth Des.* **2011**, *11*, 231–239.
- (78) Wang, Y.; Zhao, H.; Li, X.; Wang, R. A Durable Luminescent Ionic Polymer for Rapid Detection and Efficient Removal of Toxic  $\text{Cr}_2\text{O}_7^{2-}$ . *J. Mater. Chem. A* **2016**, *4*, 12554–12560.
- (79) Zhao, H.; Li, L.; Wang, Y.; Wang, R. Shape-Controllable Formation of Poly-Imidazolium Salts for Stable Palladium N-Heterocyclic Carbene Polymers. *Sci. Rep.* **2014**, *4*, 5478.
- (80) Liu, T.-T.; Liang, J.; Huang, Y.-B.; Cao, R. A Bifunctional Cationic Porous Organic Polymer Based on a Salen-(Al) Metalloligand for the Cycloaddition of Carbon Dioxide to Produce Cyclic Carbonates. *Chem. Commun.* **2016**, *52*, 13288–13291.
- (81) Samanta, P.; Chandra, P.; Dutta, S.; Desai, A. V.; Ghosh, S. K. Chemically Stable Ionic Viologen-Organic Network: an Efficient Scavenger of Toxic Oxo-Anions from Water. *Chem. Sci.* **2018**, *9*, 7874–7881.
- (82) Yoon, I.-H.; Meng, X.; Wang, C.; Kim, K.-W.; Bang, S.; Choe, E.; Lippincott, L. Perchlorate Adsorption and Desorption on Activated Carbon and Anion Exchange Resin. *J. Hazard. Mater.* **2009**, *164*, 87–94.
- (83) Wang, Y.; Gao, B.-y.; Yue, W.-w.; Yue, Q.-y. Preparation and Utilization of Wheat Straw Anionic Sorbent for the Removal of Nitrate from Aqueous Solution. *J. Environ. Sci.* **2007**, *19*, 1305–1310.